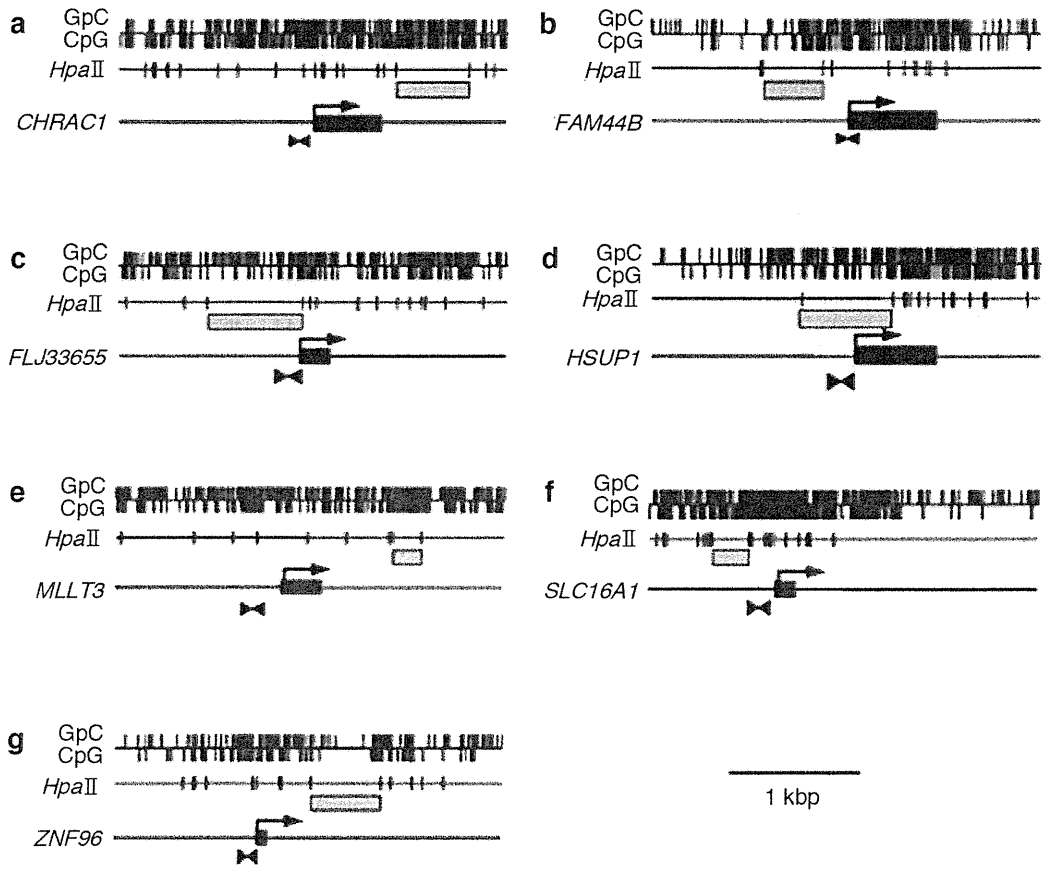

Fig. 1 Genomic structures around the seven analyzed CGIs in uterine leiomyomas. Vertical ticks show individual GpC sites (top), CpG sites (middle), and recognition sites (bottom) of restriction enzyme used for MS-RDA (HpaII). Gray boxes, DNA fragments isolated by MS-RDA; closed boxes, exons; arrowheads, MSP primers and arrows, transcription start sites and transcription directions.

tion in promoter regions (Table 1). These genes have not yet been reported that aberrantly methylated in any human tumors. MSP for 5 leiomyoma patients did not reveal aberrant promoter methylation in 7 genes (Fig. 2). These results permit two interpretations in this study. First, the isolated genes sporadically methylated in some CpG sites (CCGG), which recognized by HpaII, but not involved in whole CGIs. Second, may be that small samples examined in this study lead us with no findings. Though, our results in this study did not confirm DNA methylated in uterine leiomyoma, it did not exclude that epigenetic mechanisms may involve in the cause and development of uterine leiomyoma.

Previous investigators have shown epigenetic alteration of DNA methylation is expressed in uterine leiomyoma [20, 37]. Li *et al.* demonstrated that DNA global hypomethylation was detected in the uterine leiomyoma tissue using DNA methyl acceptance assay and immunohistochemistry staining with 5-methylcytidine antibody [20]. On the other hand, they also successfully screened two hypermethylated DNA fragments in uterine leiomyomas (NCBI access No. AZ081761 and No. AZ081762) [38]. As in cancer cells, global hypomethylation and local gene-specific hypermethylation can both be simultaneously expressed in uterine leiomyomas even though they are classified as a benign uterine disease.

Because over-expressions of estrogen-associated genes and various growth factors with mitogenic activity play a crucial role in prompting the growth of uterine leiomyomas [6], Li *et al.* postulated that the DNA global hypomethylation mechanism could contribute to elevating the expression of estrogen-associated genes and growth factors [20]. Gloudemans *et al.* also observed an inverse correlation between CpG methylation and expression of the insulin-like growth factor II (IGF-II) gene in malignant smooth muscle tissues [37]. In normal smooth muscle and in leiomyomas the IGF-II gene appeared to be methylated, while in leiomyosarcomas with IGF-II gene expression increasing, the overall methylation of IGF-II gene tended to be low or absent. MS-RDA can also identify the extensive hypomethylation of repetitive sequences, such as LINE1 [39]. In this study, we used myoma tissue DNA as driver, normal adjacent myometria DNA as tester, we cold not identify the hypomethylated DNA sequence in the leiomyoma. However, using the former DNA as tester, the latter DNA as driver should be possible to identify the hypomethylated DNA in the leiomyma.

On the other hand, increased DNMT1 and

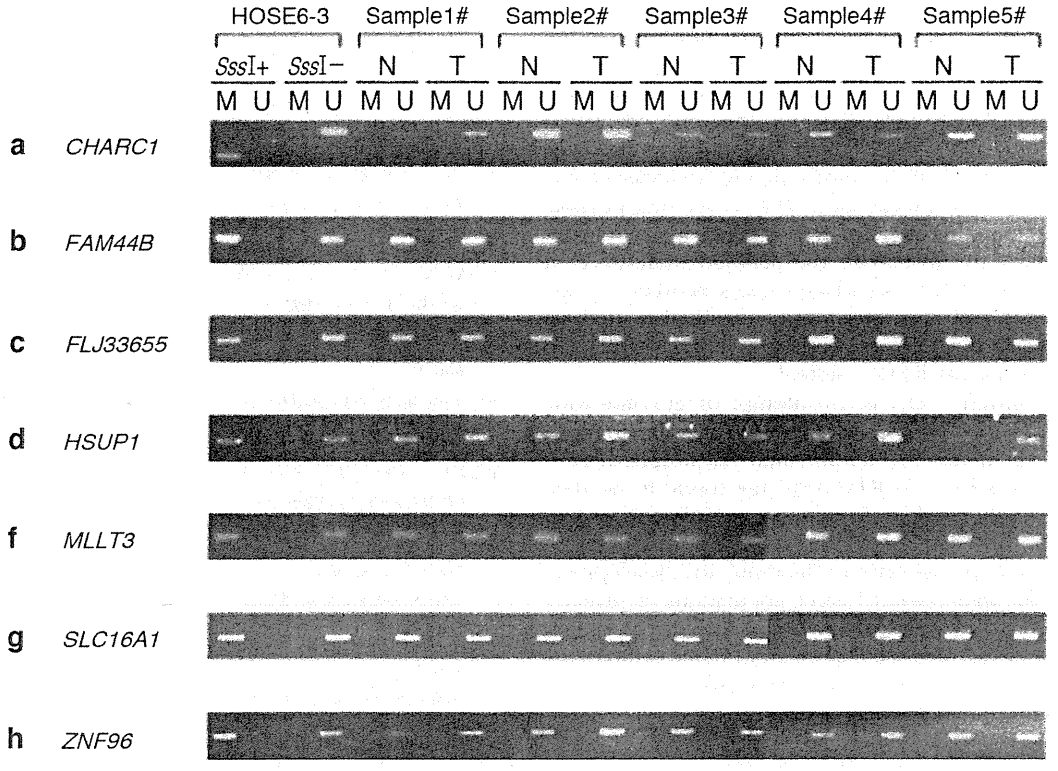

Fig. 2 Results of MSP for methylation analysis of 7 genes in 5 patients. HOSE 6-3: immortalized normal human ovarian surface epithelial cells; SssI+ : genomic DNA methylated by SssI methylase as fully methylated DNA control; SssI: genomic DNA not treated by SssI methylase as negative control. Samples 1-5: primary leiomyoma patients. N and T: normal adjacent myometria and tumor tissue, respectively. U and M: primer sets specific to unmethylated and methylated DNA molecules, respectively. No aberrant DNA methylation was found in 5 patients when analyzed for promoter methylation status of seven genes by MSP.

decreased DNMT3A and 3B expression were also revealed in uterine leiomyomas [20]. The DNMT family of enzymes catalyze the transfer of a methyl group to DNA. DNMT1 is responsible for maintenance and de novo DNA methylation, while DNMT3A and 3B are responsible for de novo DNA methylation, which refer to adding a new methyl group to unmethylated CpG sites [40]. It was reported that the expression of DNMT1, DNMT3A and 3B was elevated consistently in some cancer cells [41, 42]. While in aged cells, it showed a decrease of DNMT1 and an increase of DNMT3B [43]. Imbalanced expression of DNMT1, DNMT3A and 3B in human leiomyomas may indicate a different mechanism or proliferation efficiency in benign tumors, aged cells, and malignant tumors [20]. Taken together, a potential epigenetic mechanism plays its roles in the development of uterine leiomyomas.

In MS-RDA, use of cell lines, which can get a homogeneous population of cells, is highly recommended [25, 26]. In the present study, because few immortalized human leiomyoma and myometrial cell lines have been established, we used genomic DNA from an identical patient (case 1), whose leiomyoma tissue was used as the driver, and the adjacent myometria was used as the tester. Uterine leiomyomas are considered as monoclonal tumors that originate from smooth muscle cells [8]. Moreover, Abe *et al.* [32] also used genomic DNA of primary samples and cell lines in their MS-RDA analysis of neuroblastomas. Therefore, that use of genomic DNA of primary MS-RDA analysis is worth attempting.

Using MS-RDA can produce an abundance of DNA fragments that are unmethylated in the tester but putative and specifically methylated in the driver. It has been calculated that 104-105 CGIs can be screened by MS-RDA when compared with tumor and normal cells, and finally can distinguish 10-40 CGIs with different methylation status in a typical analysis [26]. We recently adopted MS-RDA technology to screen for CGIs aberrantly methylated in ovarian cancers, and isolated 33 CGIs that may be putative hypermethylation, and eventually successfully identified PRTFDC1 silencing and aberrant promoter methylation of GPR150, ITGA8, and HOXD11 in ovarian cancers [33]. In this study, we sequenced 192 clones and isolated 7 genes that putative aberrantly methylated in CGIs, but MSP did not find methyalted DNA in 5 primary uterine leiomyomas. Recently, Yamagata *et al.* demonstrated not only aberrant genome-wide DNA methylation status in uterine leiomyomas but

also the existence of a genomic locus that is differently methylated between normal myometrium and uterine leiomyoma using another genome-wide DNA methylation screening method, restriction landmark genomic scanning (RLGS) [44]. However, they only identified a new putative gene, GS20656, which showed an aberrant methylation status in uterine leiomyoma compared with myometrium [44]. It seemed possible that DNA methylation patterns differ among individuals. Therefore, to clarify the detailed difference in genome-wide DNA methylation status between uterine leiomyoma and normal myometrium, further analyses with larger samples are warranted using neither the MS-RDA nor the RLGS method.

In summary, this is an attempt of genome-wide screening to identify aberrant DNA methylation by MS-RDA in uterine leiomyoma. Although these 7 genes isolated by MS-RDA were not found to be aberrantly methylated in 5 primary samples, that does not rule out that epigenetic modifications of DNA methylation are involved in the cause and development of uterine leiomyomas. Larger populations of primary samples and more attempts using cell lines or primary monolayer cultures established from tissue samples are warranted to further elucidate these issues.

ACKNOWLEDGMENTS

The authors thank Prof. Sai Wah Tsao, of the University of Hong Kong, for providing HOSE6-3 cells. This study was supported by a Grant-in-Aid for the Third-Term Comprehensive 10-Year Strategy for Cancer Control from the Ministry of Health, Labour and Welfare, Japan. We also thank Robert E. Brandt, CEO, MedEd Japan, for editing the manuscript.

REFERENCES

1) Buttram VC Jr, Reiter RC. Uterine leiomyomata: etiology, symptomatology, and management. Fertil Steril 1981; 36:433-45.
2) Hart R, Khalaf Y, Yeong CT, Seed P, Taylor A, Braude P. A prospective controlled study of the effect of intramural uterine fibroids on the outcome of assisted conception. Hum Reprod 2001; 16: 2411-7.
3) Vollenhoven BJ, Lawrence AS, Healy DL. Uterine fibroids: a clinical review. Br J Obstet Gynaecol 1990; 97: 285-98.
4) Nibert M, Heim S. Uterine leiomyoma cytogenetics. Genes Chromosomes Cancer 1990; 2: 3-13.
5) Stewart EA. Uterine fibroids. Lancet 2001; 357:293-8.
6) Flake GP, Andersen J, Dixon D. Etiology and pathogenesis of uterine leiomyomas: a review. Environ Health Perspect 2003; 111: 1037-54.
7) Maruo T, Matsuo H, Shimomura Y, Kurachi O, Gao Z, Nakago S, *et al.* Effects of progesterone on growth factor expression in human uterine leiomyoma. Steroids 2003; 68: 817-24.
8) Fletcher JA, Morton CC, Pavelka K, Lage JM. () Chromosome aberrations in uterine smooth muscle tumors: potential diagnostic relevance of cytogenetic instability. Cancer Res 1990; 50: 4092-7.
9) Stewart EA, Morton CC. The genetics of uterine leiomyomata: what clinicians need to know. Obstet Gynecol 2006; 107: 917-21.
10) Rein MS, Barbieri RL, Friedman AJ. Progesterone: a critical role in the pathogenesis of uterine myomas. Am J Obstet Gynecol 1995; 172: 14-8.
11) Mangrulkar RS, Ono M, Ishikawa M, Takashima S, Klagsbrun M, Nowak RA. Isolation and characterization of heparin-binding growth factors in human leiomyomas and normal myometrium. Biol Reprod 1995; 53: 636-46.
12) Maruo T, Ohara N, Wang J, Matsuo H. Sex steroidal regulation of uterine leiomyoma growth and apoptosis. Hum Reprod Update 2004; 10: 207-20.
13) Buttram VC Jr. Uterine leiomyomata—actiology, symptomatology and management. Prog Clin Biol Res 1986; 225: 275-96.
14) Jones PA, Baylin SB. The fundamental role of epigenetic events in cancer. Nat Rev Genet 2002; 3: 415-28.
15) Herman JG, Baylin SB. Gene silencing in cancer in association with promoter hypermethylation. N Engl J Med 2003; 349: 2042-54.
16) Hsieh CJ, Klump B, Holzmann K, Borchard F, Gregor M, Porschen R. Hypermethylation of the p16INK4a promoter in colectomy specimens of patients with long-standing and extensive ulcerative colitis. Cancer Res 1998; 58: 3942-5.
17) Maekita T, Nakazawa K, Mihara M, Nakajima T, Yanaoka K, Iguchi M, *et al.* High levels of aberrant DNA methylation in Helicobacter pylori-infected gastric mucosae and its possible association with gastric cancer risk. Clin Cancer Res 2006; 12: 989-95.
18) Jurgens B, Schmitz-Drager BJ, Schulz WA. Hypomethylation of L1 LINE sequences prevailing in human urothelial carcinoma. Cancer Res 1996; 56: 5698-703.
19) Chen CH, Shih HH, Wang-Wuu S, Tai JJ, Wuu KD. Chromosomal fragile site expression in lymphocytes from patients with schizophrenia. Hum Genet 1998; 103: 702-6.
20) Li S, Chiang TC, Richard-Davis G, Barrett JC, McLachlan JA. DNA hypomethylation and imbalanced expression of DNA methyltransferases (DNMT1, 3A, and 3B) in human uterine leiomyoma. Gynecol Oncol 2003; 90: 123-30.
21) Seidel C, Bartel F, Rastetter M, Barrett JC, Mclachlan JA. Alterations of cancer-related genes in soft tissue sarcomas: hypermethylation of RASSF1A is frequently detected in leiomyosarcoma and associated with poor prognosis in sarcoma. Int J Cancer 2005; 114: 442-7.
22) Kawaguchi K, Oda Y, Saito T, Yamamoto H, Yamamoto H, Tamiya S, Takahira T, *et al.* () Mechanisms of inactivation of the p16INK4a gene in leiomyosarcoma of soft tissue: decreased p16 expression correlates with promoter methylation and poor prognosis. J Pathol 2003; 201: 487-95.
23) Kawaguchi K, Oda Y, Saito T, Yamamoto H, Takahira T, Tamiya S, *et al.* Death-associated protein kinase (DAP kinase) alteration in soft tissue leiomyosarcoma: Promoter methylation or homozygous deletion is associated with a loss of DAP kinase expression. Hum Pathol 2004; 35: 1266-71.
24) Ushijima T, Morimura K, Hosoya Y, Okonogi H, Tatematsu M, Sugimura T, *et al.* Establishment of methylation-sensitive-representational difference analysis and isolation of hypo- and hypermethylated genomic fragments in mouse liver tumors. Proc Natl Acad Sci U S A 1997; 94: 2284-9.
25) Kaneda A, Takai D, Kaminishi M, Okochi E, Ushijima T. Methylation-sensitive representational difference analysis and its application to cancer research. Ann N Y Acad Sci 2003; 983: 131-41.
26) Ushijima T. Detection and interpretation of altered methylation patterns in cancer cells. Nat Rev Cancer 2005; 5: 223-31.
27) Takai D, Yagi Y, Wakazono K, Ohishi N, Morita Y, Sugimura T, *et al.* Silencing of HTR1B and reduced expression of EDN1 in human lung cancers, revealed by methylation-sensitive representational difference analysis. Oncogene 2001; 20: 7505-13.
28) Kaneda A, Kaminishi M, Yanagihara K, Sugimura T, Ushijima T. Identification of silencing of nine genes in human gastric cancers. Cancer Res 2002; 62: 6645-50.
29) Hagihara A, Miyamoto K, Furuta J, Hiraoka N, Wakazono K, Seki S, *et al.* Identification of 27 5' CpG islands aberrantly methylated and 13 genes silenced in human pancreatic cancers. Oncogene 2004; 23: 8705-10.
30) Miyamoto K, Asada K, Fukutomi T, Okochi E, Yagi Y, Hasegawa T, *et al.* Methylation-associated silencing of heparan sulfate D-glucosaminyl 3-O-sulfotransferase-2 (3-OST-2) in human breast, colon, lung and pancreatic cancers. Oncogene 2003; 22: 274-80.
31) Miyamoto K, Fukutomi T, Akashi-Tanaka S, Hasegawa T, Asahara T, Sugimura T, *et al.* Identification of 20 genes aberrantly methylated in human breast cancers. Int J Cancer 2005; 116: 407-14.
32) Abe M, Ohira M, Kaneda A, Yagi Y, Yamamoto S, Kitano Y, *et al.* CpG island methylator phenotype is a strong determinant of

poor prognosis in neuroblastomas. Cancer Res 2005; 65: 828-34.
33) Cai LY, Abe M, Izumi S, Imura M, Yasugi T, Ushijima T. Identification of PRTFDC1 silencing and aberrant promoter methylation of GPR150, ITGA8 and HOXD11 in ovarian cancers. Life Sci 2007; 80: 1458-65.
34) Herman JG, Graff JR, Myohanen S, Nelkin BD, Baylin SB. Methylation-specific PCR: a novel PCR assay for methylation status of CpG islands. Proc Natl Acad Sci U S A 1996; 93: 9821-6.
35) Jones PA, Baylin SB. The fundamental role of epigenetic events in cancer. Nat Rev Genet 2002; 3: 415-28.
36) Herman JG, Baylin SB. Gene silencing in cancer in association with promoter hypermethylation. N Engl J Med 2003; 349: 2042-54.
37) Gloudemans T, Pospiech I, Van Der Ven LT, Lips CJ, Schneid H, Den Otter W, *et al.* Expression and CpG methylation of the insulin-like growth factor II gene in human smooth muscle tumors. Cancer Res 1992; 52: 6516-21.
38) Li S, McLachlan JA. Estrogen-associated genes in uterine leiomyoma. Ann N Y Acad Sci 2001; 948: 112-20.
39) Takai D, Yagi Y, Habib N, Sugimura T, Ushijima T. Hypomethylation of LINE1 retrotransposon in human hepatocellular carcinomas, but not in surrounding liver cirrhosis. Jpn J Clin Oncol. 2000; 30: 306-9.
40) Bheemanaik S, Reddy YV, Rao DN. Structure, function and mechanism of exocyclic DNA methyltransferases. Biochem J 2006; 399: 177-90.
41) Robertson KD, Uzvolgyi E, Liang G, Talmadge C, Sumegi J, Gonzales FA, Jones PA. The human DNA methyltransferases (DNMTs) 1, 3a and 3b: coordinate mRNA expression in normal tissues and overexpression in tumors. Nucleic Acids Res. 1999; 27: 2291-8.
42) Mizuno S, Chijiwa T, Okamura T, Akashi K, Fukumaki Y, Niho Y, *et al.* Expression of DNA methyltransferases DNMT1, 3A, and 3B in normal hematopoiesis and in acute and chronic myelogenous leukemia. Blood 2001; 97: 1172-9.
43) Lopatina N, Haskell JF, Andrews LG, Poole JC, Saldanha S, Tollefsbol T. Differential maintenance and de novo methylating activity by three DNA methyltransferases in aging and immortalized fibroblasts. J Cell Biochem 2002; 84: 324-34.
44) Yamagata Y, Maekawa R, Asada H, Taketani T, Tamura I, Tamura H, *et al.* Aberrant DNA methylation status in human uterine leiomyoma. Mol Hum Reprod 2009; 15: 259-67.

Cancer Science
The official journal of the Japanese Cancer Association JCA

Methylation silencing of angiopoietin-like 4 in rat and human mammary carcinomas

Naoko Hattori, Eriko Okochi-Takada, Mizuho Kikuyama, Mika Wakabayashi, Satoshi Yamashita and Toshikazu Ushijima[1]

Division of Epigenomics, National Cancer Center Research Institute, Tokyo, Japan

(Received January 6, 2011/Revised March 30, 2011/Accepted April 1, 2011/Accepted manuscript online April 12, 2011/Article first published online May 12, 2011)

Aberrant DNA methylation is deeply involved in the development and progression of human breast cancers, but its inducers and molecular mechanisms are still unclear. To reveal such inducers and clarify the molecular mechanisms, animal models are indispensable. Here, to identify genes silenced by promoter DNA methylation in rat mammary carcinomas, we took a combined approach of methylated DNA immunoprecipitation (MeDIP)–CpG island (CGI) microarray analysis and expression microarray analysis after treatment with epigenetic drugs. MeDIP-CGI microarray revealed that among 5031 genes with promoter CGI, 465 were methylated in a carcinoma cell line induced by 2-amino-1-methyl-6-phenylimidazo[4,5-*b*]pyridine (PhIP), but not in normal mammary epithelial cells. By treatment of the cell line with 5-aza-2′-deoxycytidine and trichostatin A, 29 of the 465 genes were shown to be re-expressed. In primary mammary carcinomas, five (*Angptl4*, *Coro1a*, *RGD1304982*, *Tmem37* and *Ndn*) of the 29 genes were methylated in one or more of 25 samples. Quantitative expression analysis revealed that *Angptl4* had high expression in normal mammary glands, but low expression in primary carcinomas. Also in humans, *ANGPTL4* was unmethylated and expressed in normal mammary epithelial cells, but was methylated in 11 of 91 (12%) primary breast cancers. This is the first study to identify genes aberrantly methylated in rat mammary carcinomas, and *Angptl4* is a novel methylation-silenced gene both in rat and human mammary carcinomas. The combination of the MeDIP-CGI microarray analysis and expression microarray analysis after treatment with epigenetic drugs was effective in reducing the number of methylated genes that are not methylation silenced. (*Cancer Sci* 2011; 102: 1337–1343)

Aberrant epigenetic modifications, such as aberrant DNA methylation and histone modifications, are deeply involved in the development and progression of human cancers.[1–3] In human breast cancers, tumor-suppressor genes, such as *RASSF1A*, *BRCA1*, *CDKN2A* and *PTEN*, are silenced by aberrant methylation of promoter CpG islands (CGI).[4] Aberrant methylation could be detected not only in cancers but also in non-cancerous breast tissues, suggesting that an epigenetic field defect is formed in breast cancer patients.[5] Despite the deep involvement of aberrant DNA methylation, limited information is available on the factors that induce aberrant methylation during mammary carcinogenesis. Among the limited information, exposure to estrogen or a nonsteroidal estrogen, bisphenol A, was reported to change the methylation status of mammary epithelial progenitor cells aberrantly *in vitro*.[6,7] However, inducers and induction mechanisms of aberrant methylation *in vivo* are still almost unknown. To address these issues, animal models are indispensable.

Rat models are useful for the study of mammary carcinogenesis in terms of several features. Mammary carcinomas can be reproducibly induced by a wide range of a selection of chemicals, including 2-amino-1-methyl-6-phenylimidazo[4,5-*b*]pyridine (PhIP),[8,9] 7,12-dimethylbenz[*a*]anthracene (DMBA)[10] and *N*-nitroso-*N*-methylurea,[11] and also by radiation,[12] and their characteristics have been well established. The induced mammary carcinomas predominantly originated from mammary ducts similar to the majority of human breast cancers.[13] As an animal model, we can use animals with a homogeneous genetic background and make any intervention to clearly analyze the effects of specific factors, such as overexposure to estrogen and intake of a high fat diet, on a phenotype. However, to analyze inducers of aberrant methylation and its mechanisms, we need genes silenced by aberrant methylation in rat mammary carcinomas, which are not known yet.

In the present study, we aimed to identify methylation-silenced genes in rat primary mammary carcinomas. To this end, we applied two genome-wide methylation analyses, methylated DNA immunoprecipitation (MeDIP)–CGI microarray analysis and expression microarray analysis after treatment with epigenetic drugs.[14]

Materials and Methods

Rat primary tissue samples and carcinoma cell lines. PhIP-induced mammary adenocarcinomas were obtained from female (F344 × SD)F1 rats at the age of 56–69 weeks who were administrated 10 doses of PhIP (75 mg/kg) at the age of 6 weeks and a high-fat diet (23.5% corn oil).[15] DMBA-induced mammary adenocarcinomas were obtained from female (F344 × SD)F1 rats at the age of 25–32 weeks who were administrated a single dose of DMBA (50 mg/kg) at the age of 7 weeks.[16] Normal mammary glands were collected from 8-week-old untreated female (F344 × SD)F1 rats and 56–69-week-old female (F344 × SD)F1 rats without administration of PhIP by the gland isolation technique for mammary ducts.[17] Primary-cultured epithelial cells were maintained as rat mammary epithelial cells (RMEC).[17] Two carcinoma cell lines, PhIP7-4 and PhIP12-1, were established from two mammary carcinomas induced by PhIP, as previously reported.[18] Two carcinoma cell lines, DMBA334 and DMBA397, were established from the DMBA-induced mammary carcinomas described above.

Human breast cancer cell lines and tissue samples. MCF-7, T47-D, SK-BR-3, MDA-MB-231, MDA-MB-468, ZR-75-1, BT-474, Hs578T and mammary epithelial cell line (MCF10A) were purchased from the American Type Culture Collection (Rockville, MD, USA). Human mammary epithelial cells (HMEC) were purchased from Cambrex (East Rutherford, NJ, USA). Human breast cancers (n = 91) and adjacent non-cancerous tissues (n = 21), which were located at least 3 cm apart from cancers, were obtained from the surgical specimens of patients who underwent mastectomy. Human samples were obtained with informed consent and the analysis was approved by the institutional review boards.

[1]To whom correspondence should be addressed. E-mail: tushijim@ncc.go.jp

doi: 10.1111/j.1349-7006.2011.01955.x

5-Aza-2′-deoxycytidine and trichostatin A treatments. PhIP7-4 cells were seeded at a density of 2×10^5 cells/10 cm plate on day 0, exposed to freshly prepared 1 or 5 μM 5-aza-2′-deoxycytidine (5-aza-dC; Sigma, St Louis, MO, USA) for 24 h on days 1 and 2, treated with 100 or 300 nM trichostatin A (TSA; Sigma) for 24 h on day 3, and then harvested on day 4. BT-474 and MDA-MB-231 cells were seeded at a density of 5×10^5 cells/6 cm plate and 6×10^5 cells/10 cm plate, respectively, on day 0, and treated with 5-aza-dC (1 or 5 μM for BT474; 0.5 or 1 μM for MDA-MB-231) for 24 h on days 1 and 3, and harvested on day 4. The doses of 5-aza-dC (and TSA) were adjusted so that the growth of treated cells is suppressed to 40–80% of non-treated cells.

MeDIP-CGI microarray analysis. As described previously,[19,20] 5 μg of sonicated DNA was immunoprecipitated with 6 μg antibody against 5-methylcytidine (Diagnode, Liége, Belgium), and the precipitated DNA and input DNA were labeled with Cy5 and Cy3, respectively. The labeled probes were hybridized to a rat CGI oligonucleotide microarray (Agilent Technologies, Santa Clara, CA, USA) that contained 93 024 probes in or within 95 bp of 13 026 CGI with an average probe spacing of 100 bp. The microarray was scanned with an Agilent G2565BA microarray scanner (Agilent Technologies), and the scanned data were processed using Feature Extraction Ver.9.1 (Agilent Technologies) and Agilent G4477AA ChIP Analytics 1.3 software (Agilent Technologies). A signal of probes was converted into a "M_e value", which represented the methylation level as a value from 0–0.3 (unmethylated) to 0.6–1 (methylated).[19] For the rat CGI microarray, the formula for the M_e value was optimized as follows: M_e value = (signal log ratio $X[1 - P(X)] - 1.3)/4.0 + 0.5$.

Definition of promoter CGI, and hierarchical clustering analysis. A CGI was defined as an assembly of probes within intervals <500 bp. A promoter CGI was defined as a CGI within a nucleosome-free region, which was defined as a region between a transcription start site (TSS) and its 200 bp upstream.[21] A TSS was determined using UCSC rn4 (Baylor Build 3.4, November 2004). According to these definitions, 5031 assemblies were defined as promoter CGI. The methylation level of a CGI was assessed by an average M_e value of the probes located within the CGI, and cut-off values of 0.6 and 0.3 were used for methylated and unmethylated CGI, respectively. Hierarchical clustering of promoter CGI by the Euclidean distance of their M_e value was performed using MultiExperimental Viewer v4.1 software (Dana-Farber Cancer Institute, Boston, MA, USA).

Oligonucleotide expression microarray analysis. Total RNA was isolated using ISOGEN (NIPPON GENE, Tokyo, Japan). Oligonucleotide microarray analysis was performed using a GeneChip Rat Genome 230 2.0 Array (Affymetrix, Santa Clara, CA, USA) with 54 000 probe sets, and 30 000 transcripts from 30 000 genes. From 7 μg of total RNA, double-stranded cDNA was synthesized and biotin-labeled cRNA was prepared using a BioArray High-Yield ENA transcript labeling kit (Enzo, Farmingdale, NY, USA). Twenty micrograms of labeled cRNA were fragmented and hybridized to the GeneChip oligonucleotide microarray. The scanned data were processed using GeneChip operating software and normalized so that the average of all genes on a GeneChip would be 500. A *P*-value for differential expression (change *P*-value) was calculated for each probe by an algorithm based on the Wilcoxon Signed-Rank test.

Methylation-specific PCR (MSP) and bisulfite sequencing. Sodium bisulfite treatment was performed as described previously using 1 μg of DNA digested with *Bam*HI (Toyobo, Tokyo, Japan),[22] and suspended in 40 μL of Tris-EDTA (TE) buffer. Fully methylated DNA was prepared by methylating genomic DNA using *Sss*I-methylase (New England Biolabs, Beverly, MA, USA). Fully unmethylated DNA was prepared by amplifying genomic DNA with ø29 DNA polymerase (GenomiPhi DNA Amplification kit; GE Healthcare UK, Buckinghamshire, UK).

Conventional MSP for screening purposes was conducted with primers specific to methylated DNA up to 39 cycles (Table S1), and samples with no PCR products amplified from methylated DNA were determined to be unmethylated samples.[22] Quantitative MSP (qMSP) was performed by real-time PCR using SYBR Green I and primers specific to methylated DNA at a locus and to a B2 repeat sequence, regardless of its methylation statuses for rat genes, or to unmethylated DNA for a human gene (Table S1). The number of DNA molecules was calculated as previously described.[23] The methylation level of a rat gene was calculated as the methylation percentage obtained as: ([number of DNA molecules methylated at a target CGI in a sample]/[number of B2 repeat in the sample])/([number of DNA molecules methylated at the target CGI in a *Sss*I-treated DNA]/[number of B2 repeat in the *Sss*I-treated DNA]) × 100; and that of a human gene as: (number of DNA molecules methylated)/([number of DNA molecules methylated] + [number of DNA molecules unmethylated]) × 100. The methylation level in a cancer sample was considered as aberrant when it was two or more times higher than the highest methylation level in normal samples.

For bisulfite sequencing, sodium bisulfite-treated DNA was amplified with primers common to methylated and unmethylated DNA sequences (Table S1). The PCR product was cloned into a pGEM-T Easy Vector (Promega, Madison, WI, USA), and 10 clones were sequenced using an ABI PRISM 310 sequencer (Applied Biosystems, Foster City, CA, USA).

Quantitative reverse transcription-PCR (qRT-PCR). DNase-treated total RNA (1 μg) was reverse-transcribed with a random hexamer (Invitrogen, Carlsbad, CA, USA) and Superscript III reverse transcriptase (Invitrogen). Quantitative PCR was carried out by real-time PCR using SYBR Green I and primers specific to genes. The primer sequences and PCR conditions are shown in Table S1. The amplification curve of a sample was compared with those of standard DNA samples with known copy numbers to obtain a copy number in the sample, as in qMSP. The number of target cDNA molecules was normalized to those of rat *Ppia* or human *GAPDH* cDNA molecules.[24]

Results

Isolation of genes methylation-silenced in a rat mammary carcinoma by integration of MeDIP-CGI microarray and expression microarray. To isolate CGI methylated in rat mammary carcinomas and identify a carcinoma with the largest number of aberrantly methylated CGI, we analyzed three primary carcinomas (PhIP7-4#1, DMBA334#1 and DMBA397#1), three carcinoma cell lines established from these primary samples, RMEC and a pool of four normal mammary glands by MeDIP-CGI microarray. Among the 5031 promoter CGI, 1745 were methylated in at least one carcinoma but not in any of the normal mammary glands. Hierarchical clustering analysis using the 1745 promoter CGI identified a group of promoter CGI methylated both in cell lines and primary carcinomas (Group A) and a group methylated mainly in carcinoma cell lines (Group B) (Fig. 1A). The number of methylated promoter CGI was the largest in the PhP7-4 cell line among the three cell lines, and 84% and 78% of the promoter CGI methylated in the DMBA334 and DMBA397 cell lines, respectively, overlapped with those in the PhIP7-4 cell line. Thus, we selected the PhIP7-4 cell line for further analysis, and isolated 465 promoter CGI methylated in this cell line but not in RMEC (Fig. 1B).

To select candidates for methylation-silenced genes, expression microarray analyses were conducted using the PhIP7-4 cell line before and after treatment with 5 μM 5-aza-dC and 100 nM TSA. The expression microarray data showed that 1705 genes

doi: 10.1111/j.1349-7006.2011.01955.x

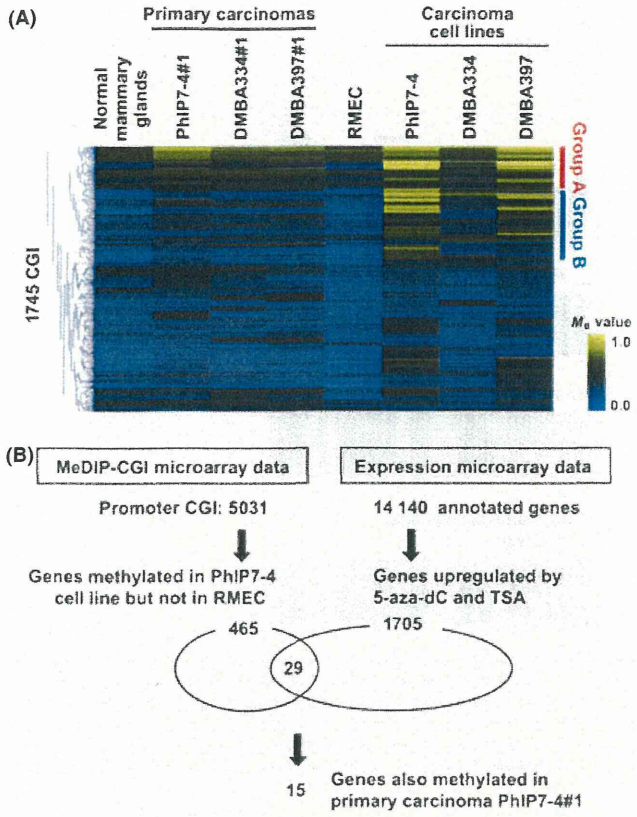

Fig. 1. Selection procedures of genes with methylated promoter CpG islands (CGI) in a rat mammary carcinoma cell line and its primary mammary carcinoma. (A) DNA methylation statuses of promoter CGI revealed by methylated DNA immunoprecipitation (MeDIP)–CGI microarray analysis. Hierarchical clustering of promoter CGI was performed using M_e values of 1745 promoter CGI methylated in at least one carcinoma and not methylated in normal mammary glands. The M_e values are represented by colors from blue (0.0) to yellow (1.0). (B) Selection procedure of genes with methylated promoter CGI in a rat mammary carcinoma cell line and then in its primary carcinoma. The number of methylated promoter CGI and that of genes upregulated by treatment of the PhIP7-4 cell line with 5-aza-2′-deoxycytidine (5-aza-dC) and trichostatin A (TSA) are shown. After integration of both sets of data, 29 candidate genes silenced in the PhIP7-4 cell line were obtained, and 15 genes were shown to be methylated also in its primary carcinoma (PhIP7-4#1). RMEC, rat mammary epithelial cells.

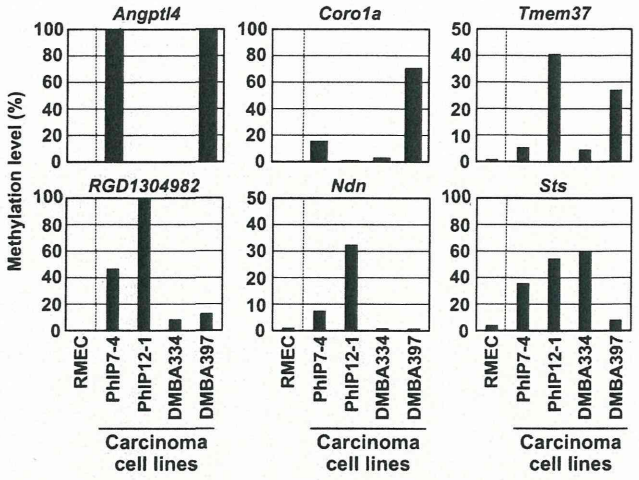

Fig. 2. Methylation levels of the six genes (*Angptl4*, *Coro1a*, *Tmem37*, *RGD1304982*, *Ndn* and *Sts*) in rat mammary carcinoma cell lines. Methylation levels of the seven genes selected by the data of methylated DNA immunoprecipitation–CpG islands (MeDIP-CGI) microarray data and expression microarray data were analyzed by quantitative methylation-specific PCR using rat mammary epithelial cells (RMEC) and the four mammary carcinoma cell lines (PhIP7-4, PhIP12-1, DMBA334 and DMBA397). Data of the six genes with high methylation levels in at least one carcinoma cell line are shown.

were upregulated twofold or more by the treatment, with *P*-values < 0.002 (Fig. 1B). By integrating the expression microarray data and the MeDIP-CGI microarray data, 29 genes were found to be methylated in the PhIP7-4 cell line and re-expressed by the epigenetic treatment. Based on the MeDIP-CGI microarray data, 14 genes methylated only in the cell line were excluded, and 15 genes methylated also in its primary tumor (PhIP7-4#1) were selected for further analysis (Fig. 1B).

Isolation of six genes methylated in rat mammary carcinoma cell lines. The data of MeDIP-microarray analysis was confirmed by conventional MSP of the PhIP7-4 cell line, and 11 of the 15 genes were methylated. Seven (*Angptl4*, *Coro1a*, *Tmem37*, *RGD1304982*, *Scin*, *Ndn* and *Sts*) of the 11 genes were not methylated in RMEC, while the remaining four were methylated (data not shown). The methylation levels of the seven genes were further quantified by qMSP in the RMEC and four carcinoma cell lines (the three cell lines used for the initial microarray analysis and PhIP12-1) (Fig. 2). Six genes (*Angptl4*, *Coro1a*, *Tmem37*, *RGD1304982*, *Ndn* and *Sts*) were highly methylated in one or more carcinoma cell lines (Fig. 2), supporting that aberrant methylation of these genes was present in epithelial cancer cells. In contrast, *Scin* had methylation levels <10% in all the carcinoma cell lines and the RMEC (data not shown).

Identification of five genes methylated in rat primary mammary carcinomas. Methylation levels of the six genes in primary carcinomas were quantified using 13 PhIP-induced primary mammary carcinomas, 12 DMBA-induced primary mammary carcinomas and seven normal mammary glands from age-matched control rats by qMSP (Fig. 3A). Two genes (*Angptl4* and *Coro1a*) were barely methylated in normal mammary glands, and were aberrantly methylated in three or more PhIP- and DMBA-induced carcinomas, showing carcinoma-specific aberrant methylation. *RGD1304982* was also barely methylated in normal mammary glands, and only one PhIP-induced carcinoma had aberrant methylation. Two genes (*Tmem37* and *Ndn*) had background methylation in normal mammary glands. *Tmem37* was aberrantly methylated in three of the 13 PhIP-induced and one of the 12 DMBA-induced carcinomas, and *Ndn* was aberrantly methylated only in two PhIP-induced carcinomas. The remaining one gene, *Sts*, was highly methylated in normal mammary glands, and carcinoma-specific methylation could not be confirmed.

The presence of dense methylation of the promoter CGI of *Angptl4* was analyzed by bisulfite sequencing of the PhIP7-4 cell line and a primary carcinoma (methylation level of 30% by qMSP) (Fig. 3B). Densely methylated DNA molecules were present in these two samples while they were absent in the RMEC and normal mammary glands (Fig. 3B).

Identification of *Angptl4* as a gene methylation silenced in rat mammary carcinomas with abundant expression in normal mammary glands. Expression in normal mammary glands was examined by qRT-PCR. *Angptl4* was highly expressed (Fig. 4A), but the other four genes (*Coro1a*, *Tmem37*, *RGD1304982* and *Ndn*) were not expressed (data not shown). *Angptl4* was not expressed in two carcinoma cell lines and

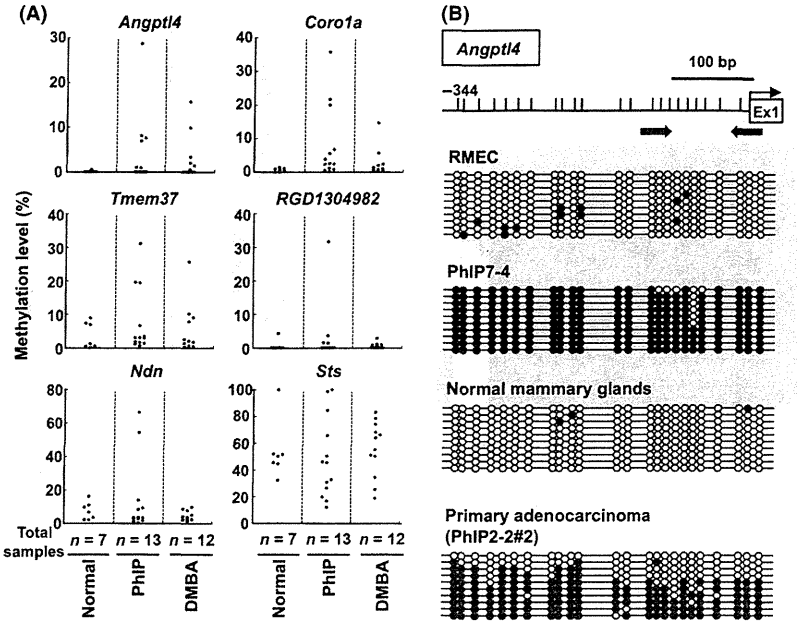

Fig. 3. Methylation of six genes in primary rat mammary carcinomas. (A) Methylation levels analyzed by quantitative methylation-specific PCR (qMSP) of seven normal mammary glands (Normal), and 13 PhIP-induced (PhIP) or 12 DMBA-induced (DMBA) primary mammary carcinomas. A carcinoma sample was considered to have aberrant methylation when its methylation level was two or more times higher than the highest methylation level in normal samples. (B) Presence of dense methylation in the PhIP7-4 cell line and a primary carcinoma, PhIP2-2#2. The methylation status of individual CpG sites (vertical lines, shown at the top) in the upstream region of *Angptl4* was determined by bisulfite sequencing. Closed circles, methylated CpG islands (CGI) sites; open circles, unmethylated CpG sites; closed arrows, location of the primers for MSP.

primary carcinomas, and unexpectedly also not in RMEC (Fig. 4A). Re-expression after the treatment of PhIP7-4 with 5-aza-dC and TSA was confirmed by qRT-PCR (Fig. 4B), supporting methylation silencing of *Angptl4*.

Methylation silencing of *ANGPTL4* in human breast cancer samples. Finally, we investigated methylation silencing of human *ANGPTL4*, which has a promoter CGI, as does rat *Angptl4*, in human breast cancers. *ANGPTL4* was expressed in two kinds of mammary epithelial cells (HMEC and MCF10A) that had unmethylated DNA (Fig. 5A). Among eight breast cancer cell lines, *ANGPTL4* was highly methylated in three cell lines (MDA-MB-231, MDA-MB-468 and BT-474), and had little expression in these cell lines (Fig. 5A). *ANGPTL4* was re-expressed by 5-aza-dC treatment of BT-474 and MDA-MB-231, showing that *ANGPTL4* was also silenced by methylation in human breast cancer cell lines (Fig. 5B).

Methylation of *ANGPTL4* was analyzed in 91 primary human breast cancers and non-cancerous breast tissues of 21 cancer patients by qMSP. Using a cut-off value of 10%,[25] methylation was detected in 11 of the 91 breast cancers (12%), while little methylation was detected in the non-cancerous tissues (Fig. 6). The methylation status in cancer was not associated with any clinicopathological characteristics, including age, clinical stage, tumor size, estrogen receptor status, progesterone receptor status, HER2 expression and recurrence (data not shown). These data showed that methylation silencing of *Angptl4* is commonly present in mammary carcinomas of both rats and humans.

Discussion

In the present study, genes with aberrant methylation of promoter CGI in rat primary mammary carcinomas were identified for the first time, and *Angptl4* was demonstrated as a novel methylation-silenced gene both in rat and human mammary carcinomas. The combination of the MeDIP-CGI microarray analysis and expression microarray analysis after epigenetic treatment was effective in reducing the number of methylated genes that were not methylation silenced.

ANGPTL4 is a secreted protein of the angiopoietin-like family, involved in lipid metabolism,[26] and upregulated by hypoxia.[27] It is known to be silenced in human gastric cancers[28] and in human melanoma cell lines.[29] The role of ANGPTL4 in mammary carcinomas remains controversial. Padua *et al.*,[30] reported that overexpression of ANGPTL4 mediated lung metastasis of estrogen receptor-negative breast cancer cells. In contrast, Foreman *et al.* and Girroir *et al.*[31,32] reported that *Angptl4* was upregulated by PPARβ/∂ activation, and inhibited growth of human and mouse mammary carcinoma cell lines. Here we found that *Angptl4* was expressed in rat mammary glands and human mammary epithelial cells, and methylation silenced in rat mammary carcinomas and human breast cancers. Together with Foreman *et al.* and Girroir *et al.* findings, *Angptl4* was suggested to be a tumor-suppressor gene.

The other four genes (*Coro1a*, *Tmem37*, *RGD1304982* and *Ndn*) were likely to have been methylated as a consequence of rat mammary carcinogenesis because they were not expressed in normal mammary glands. However, several interesting features have been reported about *Ndn* and *RGD1304982*. Human *NDN* is reported to suppress the growth of osteosarcoma cells, have anti-angiogenic effects both *in vitro* and *in vivo*, and interact with tumor suppressor p53.[33,34] A putative quinone oxidoreductase-like protein 2, encoded by *RGD1304982*, has homology to human NAD(P)H:quinone oxidoreductase 1 (*NQO1*) and NRH:quinone oxidoreductase 2 (*NQO2*), which are known to stabilize p53.[35] The possibility remains that *Ndn* and *RGD1304982* expression is induced in response to cellular stresses in normal mammary glands, and that these two genes function as tumor suppressors.

doi: 10.1111/j.1349-7006.2011.01955.x

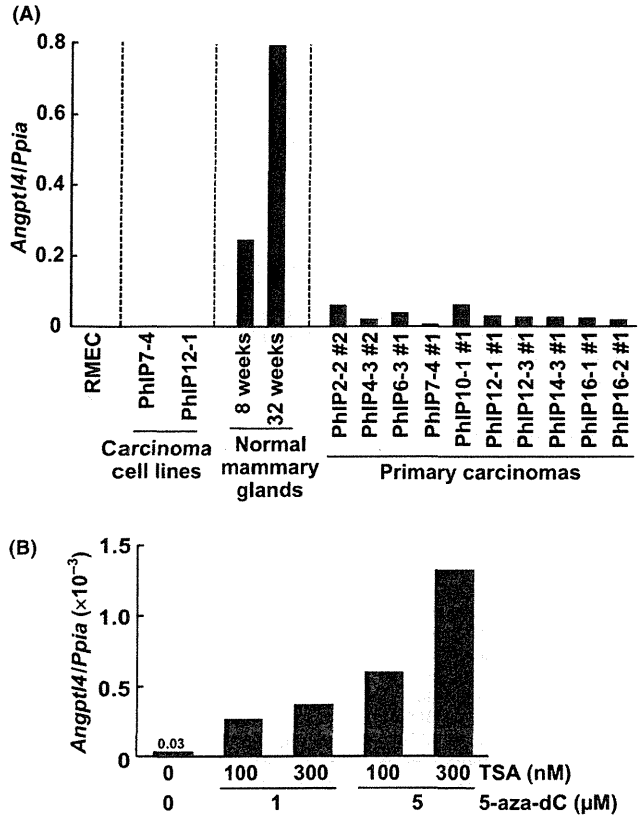

Fig. 4. Expression analysis of rat *Angptl4*. (A) *Angptl4* expression in rat mammary epithelial cells (RMEC), normal mammary glands, carcinoma cell lines (PhIP7-4 and PhIP12-1) and 10 PhIP-induced primary carcinomas analyzed by qRT-PCR. *Angptl4* expression was lost in the cell lines, and decreased in all the carcinomas. (B) Re-expression of *Angptl4* after epigenetic treatment of PhIP7-4 cells with 5-aza-2′-deoxycytidine (5-aza-dC) and trichostatin A (TSA). *Angptl4* re-expression was confirmed.

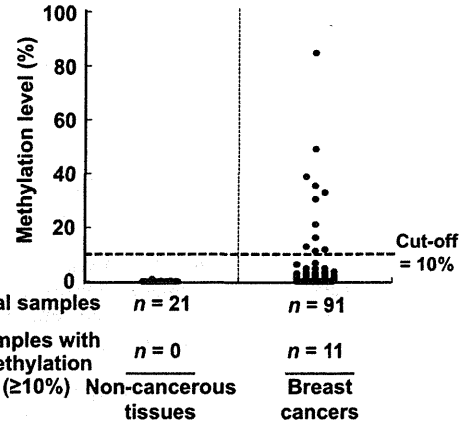

Fig. 6. Methylation levels of human *ANGPTL4* obtained by quantitative methylation-specific PCR (qMSP) of primary human tissue samples. Methylation was barely observed in non-cancerous tissues, but high methylation levels were observed in breast cancer tissues. Using a threshold of 10%, 11 cancers showed aberrant methylation.

Two (*Tmem37* and *Ndn*) of the five genes aberrantly methylated in mammary carcinomas were slightly methylated in normal-appearing mammary glands of old rats (56–69 weeks old) (Fig. 3A), which did not contain cancerous tissues. This aberrant methylation was not observed in mammary glands of young rats (8 weeks old) (data not shown), suggesting that these two genes are methylated in an age-dependent manner. It is known that age-dependent methylation can be accelerated by inflammation in the colon,[36] and there is a possibility that these genes can be used as efficient markers to assess the effects of possible inducers of aberrant methylation during mammary carcinogenesis.

Four rat primary carcinomas and two human breast cancer cell lines (T-47D and Hs578T) did not express *ANGPTL4*, although their DNA was unmethylated (Figs 4A, 5A). It is frequently observed that a gene methylation silenced in some cancer cell lines is not expressed in other cell lines by mechanisms other than CGI methylation, such as loss of transcription factors or signal dysregulation.[37] In the case of *ANGPTL4*, its expression is known to be stimulated by TGFß signaling,[30] which is disrupted in various kinds of cancers. *Angptl4* was not expressed even in RMEC (Fig. 4A), suggesting that under *in vitro* culture conditions factors required for *ANGPTL4* expression are lacking.

Methodologically, we integrated the MeDIP-CGI microarray data and those by expression microarray analysis after epigenetic treatment to identify methylation-silenced genes. The integration effectively reduced the number of candidate genes from

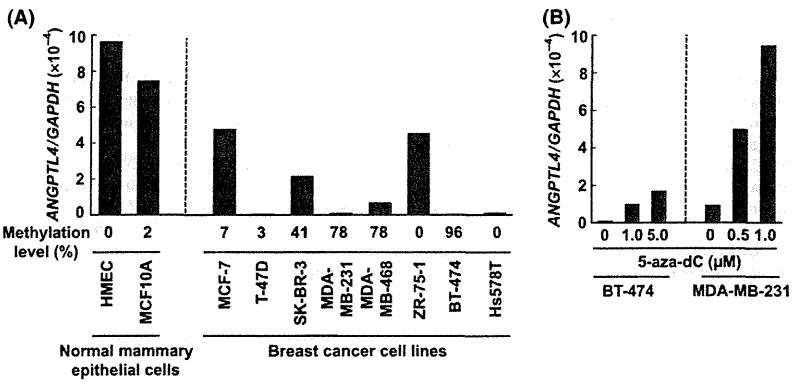

Fig. 5. Methylation silencing of human *ANGPTL4*. (A) Expression levels of human *ANGPTL4* in normal mammary epithelial cells and cancer cell lines by qRT-PCR, along with its methylation levels by qMSP. *ANGPTL4* expression was very low in the three cell lines (MDA-MB-231, MDA-MB-468 and BT-474) with high methylation levels. (B) Re-expression of *ANGPTL4* after treatment of breast cancer cell lines (BT-474 and MDA-MB-231) with 5-aza-2′-deoxycytidine (5-aza-dC).

465 (by the MeDIP-CGI microarray analysis) and 1705 (by the expression microarray analysis) after epigenetic treatment) to 29 genes. The MeDIP-CGI microarray can isolate methylated CGI, but these are not always located in genomic regions important for gene silencing.[19] The expression microarray analysis after epigenetic treatment, also known as chemical genomic screening[14,38] or pharmacological unmasking,[39] is a simple and cost-effective method in identifying methylation-silenced genes using cell lines.[14,29,38] However, genes isolated by this method are known to contain many genes that were induced by the actions of 5-aza-dC other than DNA demethylation, such as activation of the p53 pathway.[40] The approach taken here is a more effective way to identify methylation-silenced genes by reducing the number of methylated genes that are not methylation silenced.

A rat CGI microarray was custom designed in the present study. Its use successfully led to identification of a novel methylation-silenced gene not only in rat but also in human mammary carcinomas. Rats are widely used in the fields of biomedical research, such as cancers, toxicology, physiology and cardiovascular diseases, and a large amount of data using rat models has been accumulated.[41,42] The rat CGI microarray can be used for various epigenetic research in rats.

In conclusion, this is the first study that identified genes aberrantly methylated in rat mammary carcinomas. *Angptl4* is a novel methylation-silenced gene both in rat and human mammary carcinomas.

Acknowledgments

N.H. is the recipient of a Research Resident Fellowship from the Foundation for Promotion of Cancer Research. This study was supported by a Grant-in-Aid for the Third-Term Comprehensive Cancer Control Strategy from the Ministry of Health, Labour and Welfare, Japan, and by the A3 Foresight Program from the Japan Society for the Promotion of Science.

Disclosure Statement

The authors have no conflict of interest.

References

1 Esteller M. Cancer epigenomics: DNA methylomes and histone-modification maps. *Nat Rev Genet* 2007; **8**: 286–98.
2 Jones PA, Baylin SB. The epigenomics of cancer. *Cell* 2007; **128**: 683–92.
3 Linhart HG, Lin H, Yamada Y *et al.* Dnmt3b promotes tumorigenesis *in vivo* by gene-specific de novo methylation and transcriptional silencing. *Genes Dev* 2007; **21**: 3110–22.
4 Hinshelwood RA, Clark SJ. Breast cancer epigenetics: normal human mammary epithelial cells as a model system. *J Mol Med* 2008; **86**: 1315–28.
5 Yan PS, Venkataramu C, Ibrahim A *et al.* Mapping geographic zones of cancer risk with epigenetic biomarkers in normal breast tissue. *Clin Cancer Res* 2006; **12**: 6626–36.
6 Cheng AS, Culhane AC, Chan MW *et al.* Epithelial progeny of estrogen-exposed breast progenitor cells display a cancer-like methylome. *Cancer Res* 2008; **68**: 1786–96.
7 Weng YI, Hsu PY, Liyanarachchi S *et al.* Epigenetic influences of low-dose bisphenol A in primary human breast epithelial cells. *Toxicol Appl Pharmacol* 2010; **248**: 111–21.
8 Ghoshal A, Preisegger KH, Takayama S *et al.* Induction of mammary tumors in female Sprague–Dawley rats by the food-derived carcinogen 2-amino-1-methyl-6-phenylimidazo[4,5-*b*]pyridine and effect of dietary fat. *Carcinogenesis* 1994; **15**: 2429–33.
9 Snyderwine EG, Thorgeirsson UP, Venugopal M *et al.* Mammary gland carcinogenicity of 2-amino-1-methyl-6-phenylimidazo[4,5-*b*]pyridine in Sprague-Dawley rats on high- and low-fat diets. *Nutr Cancer* 1998; **31**: 160–7.
10 Russo J, Tay LK, Ciocca DR *et al.* Molecular and cellular basis of the mammary gland susceptibility to carcinogenesis. *Environ Health Perspect* 1983; **49**: 185–99.
11 Sukumar S, McKenzie K, Chen Y. Animal models for breast cancer. *Mutat Res* 1995; **333**: 37–44.
12 Imaoka T, Nishimura M, Iizuka D *et al.* Radiation-induced mammary carcinogenesis in rodent models: what's different from chemical carcinogenesis? *J Radiat Res (Tokyo)* 2009; **50**: 281–93.
13 Russo J, Russo IH. Atlas and histologic classification of tumors of the rat mammary gland. *J Mammary Gland Biol Neoplasia* 2000; **5**: 187–200.
14 Suzuki H, Gabrielson E, Chen W *et al.* A genomic screen for genes upregulated by demethylation and histone deacetylase inhibition in human colorectal cancer. *Nat Genet* 2002; **31**: 141–9.
15 Okochi E, Watanabe N, Sugimura T *et al.* Single nucleotide instability: a wide involvement in human and rat mammary carcinogenesis? *Mutat Res* 2002; **507**: 101–11.
16 Kuramoto T, Morimura K, Yamashita S *et al.* Etiology-specific gene expression profiles in rat mammary carcinomas. *Cancer Res* 2002; **62**: 3592–7.
17 Okochi E, Watanabe N, Shimada Y *et al.* Preferential induction of guanine deletion at 5′-GGGA-3′ in rat mammary glands by 2-amino-1-methyl-6-phenylimidazo[4,5-*b*]pyridine. *Carcinogenesis* 1999; **20**: 1933–8.
18 Watanabe N, Okochi E, Hirayama Y *et al.* Single nucleotide instability without microsatellite instability in rat mammary carcinomas. *Cancer Res* 2001; **61**: 2632–40.
19 Yamashita S, Hosoya K, Gyobu K *et al.* Development of a novel output value for quantitative assessment in methylated DNA immunoprecipitation-CpG island microarray analysis. *DNA Res* 2009; **16**: 275–86.
20 Takeshima H, Yamashita S, Shimazu T *et al.* The presence of RNA polymerase II, active or stalled, predicts epigenetic fate of promoter CpG islands. *Genome Res* 2009; **19**: 1974–82.
21 Yuan GC, Liu YJ, Dion MF *et al.* Genome-scale identification of nucleosome positions in *S. cerevisiae*. *Science* 2005; **309**: 626–30.
22 Yamashita S, Takahashi S, McDonell N *et al.* Methylation silencing of transforming growth factor-beta receptor type II in rat prostate cancers. *Cancer Res* 2008; **68**: 2112–21.
23 Niwa T, Tsukamoto T, Toyoda T *et al.* Inflammatory processes triggered by *Helicobacter pylori* infection cause aberrant DNA methylation in gastric epithelial cells. *Cancer Res* 2010; **70**: 1430–40.
24 Weisinger G, Gavish M, Mazurika C *et al.* Transcription of actin, cyclophilin and glyceraldehyde phosphate dehydrogenase genes: tissue- and treatment-specificity. *Biochim Biophys Acta* 1999; **1446**: 225–32.
25 Terada K, Okochi-Takada E, Akashi-Tanaka S *et al.* Association between frequent CpG island methylation and *HER2* amplification in human breast cancers. *Carcinogenesis* 2009; **30**: 466–71.
26 Mandard S, Zandbergen F, van Straten E *et al.* The fasting-induced adipose factor/angiopoietin-like protein 4 is physically associated with lipoproteins and governs plasma lipid levels and adiposity. *J Biol Chem* 2006; **281**: 934–44.
27 Le Jan S, Amy C, Cazes A *et al.* Angiopoietin-like 4 is a proangiogenic factor produced during ischemia and in conventional renal cell carcinoma. *Am J Pathol* 2003; **162**: 1521–8.
28 Kaneda A, Kaminishi M, Yanagihara K *et al.* Identification of silencing of nine genes in human gastric cancers. *Cancer Res* 2002; **62**: 6645–50.
29 Nobeyama Y, Okochi-Takada E, Furuta J *et al.* Silencing of tissue factor pathway inhibitor-2 gene in malignant melanomas. *Int J Cancer* 2007; **121**: 301–7.
30 Padua D, Zhang XH, Wang Q *et al.* TGFbeta primes breast tumors for lung metastasis seeding through angiopoietin-like 4. *Cell* 2008; **133**: 66–77.
31 Foreman JE, Sharma AK, Amin S *et al.* Ligand activation of peroxisome proliferator-activated receptor-beta/delta (PPARbeta/delta) inhibits cell growth in a mouse mammary gland cancer cell line. *Cancer Lett* 2009; **288**: 219–25.
32 Girroir EE, Hollingshead HE, Billin AN *et al.* Peroxisome proliferator-activated receptor-beta/delta (PPARbeta/delta) ligands inhibit growth of UACC903 and MCF7 human cancer cell lines. *Toxicology* 2008; **243**: 236–43.
33 Shibui T, Higo Y, Tsutsui TW *et al.* Changes in expression of imprinted genes following treatment of human cancer cell lines with non-mutagenic or mutagenic carcinogens. *Int J Oncol* 2008; **33**: 351–60.
34 Taniura H, Kobayashi M, Yoshikawa K. Functional domains of necdin for protein-protein interaction, nuclear matrix targeting, and cell growth suppression. *J Cell Biochem* 2005; **94**: 804–15.
35 Gong X, Kole L, Iskander K *et al.* NRH:quinone oxidoreductase 2 and NAD(P)H:quinone oxidoreductase 1 protect tumor suppressor p53 against 20s proteasomal degradation leading to stabilization and activation of p53. *Cancer Res* 2007; **67**: 5380–8.
36 Issa JP, Ahuja N, Toyota M *et al.* Accelerated age-related CpG island methylation in ulcerative colitis. *Cancer Res* 2001; **61**: 3573–7.
37 Fatemi M, Pao MM, Jeong S *et al.* Footprinting of mammalian promoters: use of a CpG DNA methyltransferase revealing nucleosome positions at a single molecule level. *Nucleic Acids Res* 2005; **33**: e176.

doi: 10.1111/j.1349-7006.2011.01955.x

38 Yamashita S, Tsujino Y, Moriguchi K *et al.* Chemical genomic screening for methylation-silenced genes in gastric cancer cell lines using 5-aza-2′-deoxycytidine treatment and oligonucleotide microarray. *Cancer Sci* 2006; **97**: 64–71.
39 Yamashita K, Upadhyay S, Osada M *et al.* Pharmacologic unmasking of epigenetically silenced tumor suppressor genes in esophageal squamous cell carcinoma. *Cancer Cell* 2002; **2**: 485–95.
40 Wang H, Zhao Y, Li L *et al.* An ATM- and Rad3-related (ATR) signaling pathway and a phosphorylation-acetylation cascade are involved in activation of p53/p21Waf1/Cip1 in response to 5-aza-2′-deoxycytidine treatment. *J Biol Chem* 2008; **283**: 2564–74.
41 Jacob HJ. Functional genomics and rat models. *Genome Res* 1999; **9**: 1013–6.
42 Toyokuni S. Iron and carcinogenesis: from Fenton reaction to target genes. *Redox Rep* 2002; **7**: 189–97.

Supporting Information

Additional Supporting Information may be found in the online version of this article:

Table S1. Primers for MSP, RT-PCR and bisulfite sequencing.

Please note: Wiley-Blackwell are not responsible for the content or functionality of any supporting materials supplied by the authors. Any queries (other than missing material) should be directed to the corresponding author for the article.

厚生労働科学研究費補助金

第３次対がん総合戦略研究事業

ヒトがんにおけるエピジェネティックな異常の解明と応用に関する研究

平成２３年度　総括・分担研究報告書

研究代表者　牛島　俊和

平成２４年（２０１２）年　４月

２／２冊

UICC
global cancer control

IJC
International Journal of Cancer

Carcinogenetic risk estimation based on quantification of DNA methylation levels in liver tissue at the precancerous stage

Ryo Nagashio[1], Eri Arai[1], Hidenori Ojima[1], Tomoo Kosuge[2], Yutaka Kondo[3] and Yae Kanai[1]

[1] Pathology Division, National Cancer Center Research Institute, Tokyo, Japan
[2] Hepatobiliary and Pancreatic Surgery Division, National Cancer Center Hospital, Tokyo, Japan
[3] Division of Molecular Oncology, Aichi Cancer Center Research Institute, Nagoya, Japan

For appropriate surveillance of patients at the precancerous stage for hepatocellular carcinomas (HCCs), carcinogenetic risk estimation is advantageous. The aim of our study was to establish criteria for such estimation based on DNA methylation profiling. The DNA methylation status of 203 CpG sites on 25 bacterial artificial chromosome (BAC) clones, whose DNA methylation status had been proven to discriminate samples of noncancerous liver tissue obtained from patients with HCC (N) from normal liver tissue (C) samples by BAC array-based methylated CpG island amplification, was evaluated quantitatively using pyrosequencing. The 45 CpG sites whose DNA methylation levels differed significantly between C and N in the learning cohort (n = 22) were identified. The criteria combining DNA methylation status for the 30 regions including the 45 CpG sites were able to diagnose N as being at high risk of carcinogenesis with 100% sensitivity and specificity in the learning cohort and 95.6% sensitivity and 100% specificity in the validation (n = 90) cohort. DNA methylation status for the 30 regions in N samples was significantly correlated with the outcome of patients with HCCs, indicating that clinicopathologically valid DNA methylation alterations have already accumulated at the precancerous stage. The DNA methylation status of the 30 regions did not depend on the presence or absence of hepatitis virus infection, or the status of noncancerous liver tissue (chronic hepatitis or cirrhosis). These criteria may be applicable for carcinogenetic risk estimation using liver biopsy specimens obtained from patients who are followed up because of chronic liver diseases.

Early Detection and Diagnosis

Hepatocellular carcinoma (HCC) is a common malignancy worldwide. Hepatitis virus infection is associated with an extremely high risk of HCC development. Although mass vaccination against hepatitis B virus (HBV) has been initiated, HBV-associated liver carcinogenesis will not be stamped out for many years, as the age at presentation of HBV is over 50 years mainly in Asia and Africa.[1] The spread of hepatitis C virus (HCV) in Japan that occurred in the 1950s and 1960s has resulted in a rapid increase in the incidence of HCC since 1980s.[2] In other countries, including the United States, HCV infection has spread more recently.[2] As HCC usually develops in liver already affected by chronic hepatitis or liver cirrhosis associated with hepatitis virus infection, the prognosis of patients with HCC is deemed poor, unless the cancer is diagnosed at an early stage. Therefore, surveillance at the precancerous stage will become a priority. In clinical practice, especially intensive surveillance should be performed on patients at high risk of HCC development, even if the patients are asymptomatic. Thus, risk estimation for HCC development is essential for the management of patients with chronic liver diseases.

Alterations of DNA methylation are among the most consistent epigenetic changes observed during multistage human carcinogenesis.[3,4] Accumulating evidence suggests that alterations of DNA methylation are involved even in the early and precancerous stages.[5,6] With respect to hepatocarcinogenesis, DNA methylation alterations associated with expression and/or splicing abnormalities of DNA methyltransferases are already present in liver tissues exhibiting chronic hepatitis or liver cirrhosis obtained from patients with HCCs.[7–11] Differing from alterations of mRNA and protein expression, which can be easily affected by the microenvironment of cancer

Key words: chronic hepatitis, hepatocellular carcinoma, liver cirrhosis, precancerous condition, pyrosequencing

Abbreviations: anti-HCV: anti-HCV antibody; BAC: bacterial artificial chromosome; BAMCA: BAC array-based methylated CpG island amplification; HBs-Ag: HBV surface antigen; HBV: hepatitis B virus; HCC: hepatocellular carcinoma; HCV: hepatitis C virus; PCR: polymerase chain reaction

Additional Supporting Information may be found in the online version of this article.

Grant sponsors: Third Term Comprehensive 10-Year Strategy for Cancer Control from the Ministry of Health, Labor and Welfare of Japan, Cancer Research from the Ministry of Health, Labor and Welfare of Japan, Program for Promotion of Fundamental Studies in Health Sciences of the National Institute of Biomedical Innovation (NiBio), Foundation for Promotion of Cancer Research in Japan
DOI: 10.1002/ijc.26061
History: Received 7 Oct 2010; Accepted 17 Feb 2011; Online 11 Mar 2011

Correspondence to: Yae Kanai, Pathology Division, National Cancer Center Research Institute, 5-1-1 Tsukiji, Chuo-ku, Tokyo 104-0045, Japan, Tel.: +81-3-3542-2511, Fax: +81-3-3248-2463, E-mail: ykanai@ncc.go.jp

cells or precursor cells, DNA methylation alterations are stably preserved on DNA double strands by covalent bonds. Therefore, even subtle alterations at the precancerous stage can be detected using highly sensitive methodology. DNA methylation alterations may be optimal indicators for carcinogenetic risk estimation.[12,13]

We have already established criteria for estimation of the risk of HCC development using bacterial artificial chromosome (BAC) array-based methylated CpG island amplification (BAMCA),[14–19] which can provide an overview of the DNA methylation tendency of individual large regions among all chromosomes;[13,19] 25 BAC clones, whose DNA methylation status was able to discriminate noncancerous liver tissue obtained from patients with HCCs in the learning cohort from normal liver tissue obtained from patients without HCCs, were identified.[18] However, sensitivity and specificity of such discrimination were not 100% in the validation cohort. Moreover, the CpG sites that are of diagnostic importance are unclear on each of the BAC clones with an average insert size of 170 kbp.[20] As the technique of BAMCA requires a large amount of genomic DNA and is somewhat cumbersome, risk estimation using BAMCA may be difficult to apply in a clinical setting.

Here, to identify precisely the CpG sites having the largest diagnostic impact, we quantitatively evaluated the DNA methylation status of 203 CpG sites on these 25 BAC clones using pyrosequencing in tissue specimens. Among the CpG sites, we were able to improve the specificity of carcinogenetic risk estimation by combining those showing the largest diagnostic impact and to apply such risk estimation to a very small amount of genomic DNA with a view to clinical application.

Material and Methods

Patients and tissue samples

As a learning cohort, 10 samples of normal liver tissue (C1–C10) showing no remarkable histological findings were obtained from specimens surgically resected from 10 patients without HCCs who were negative for both HBV surface antigen (HBs-Ag) and anti-HCV antibody (anti-HCV). The patients comprised seven men and three women with a mean (± standard deviation) age of 58.4 ± 9.7 years. Nine patients underwent partial hepatectomy for liver metastases of primary colon cancer, and one patient did so for liver metastases of a gastrointestinal stromal tumor of the stomach at the National Cancer Center Hospital, Tokyo, Japan. A total of 12 samples of noncancerous liver tissue (N1–N12) were obtained from 12 patients who underwent partial hepatectomy for HCCs. These patients comprised nine men and three women with a mean age of 65.3 ± 6.4 years. Among them, six were positive for HBs-Ag and six were positive for anti-HCV. Histological examination of these noncancerous liver tissue samples revealed findings compatible with chronic hepatitis in four and cirrhosis in eight.

As a validation cohort, 45 samples of normal liver tissue (C11–C55) exhibiting no remarkable histological findings were obtained from 45 patients without HCCs who were negative for both HBs-Ag and anti-HCV. The patients comprised 34 men and 11 women with a mean age of 62.2 ± 7.0 years. A total of 39 patients underwent partial hepatectomy for liver metastases from primary colon cancer, three patients did so for liver metastasis from gastric cancer and the remaining three patients did so for liver metastasis from each of gastrointestinal stromal tumor of the stomach, pancreatic cancer and colon carcinoid tumor, respectively. A total of 45 samples of noncancerous liver tissue (N13–N57) were obtained from 45 patients who underwent partial hepatectomy for HCCs. The patients comprised 37 men and eight women with a mean age of 62.3 ± 9.7 years. Of them 13 were positive for HBs-Ag, 29 were positive for anti-HCV, and three were negative for both. Histological examination of these noncancerous liver tissue samples revealed findings compatible with chronic hepatitis in 22 and cirrhosis in 23.

For comparison, 34 samples of primary HCC (T1–T34) were also obtained from specimens surgically resected from the patients who had provided the samples N1–N34. In addition, for comparison, 14 samples of liver tissue (V1–V14) were obtained from 14 patients who were positive for HBs-Ag or anti-HCV, but who had never developed HCCs. The patients comprised six men and eight women with a mean age of 65.1 ± 8.2 years. Of them, 12 patients underwent partial hepatectomy for liver metastases of primary colorectal cancer and two patients did so for liver metastases of gastric cancer.

Our study was approved by the Ethics Committee of the National Cancer Center, Tokyo, Japan. All the patients gave informed consent before their inclusion in our study.

DNA extraction and bisulfite DNA modification

High-molecular-weight DNA from fresh-frozen tissue samples was extracted using phenol–chloroform followed by dialysis. Bisulfite conversion was carried out using 1 μg of genomic DNA and the reagents provided in the EpiTect Bisulfite Kit (QIAGEN GmbH, Hilden, Germany), in accordance with the manufacturer's protocol. This process converts unmethylated cytosine residues to uracil, whereas methylated cytosine residues remain unchanged.[21]

Pyrosequencing DNA methylation analysis

DNA methylation level was measured by a highly quantitative method using Pyrosequencing™ technology. Polymerase chain reaction (PCR) and sequencing primers were designed based on the converted sequences using Pyrosequencing Assay Design Software ver.1.0 (QIAGEN GmbH). To overcome PCR bias in DNA methylation analysis, we optimized the annealing temperature as described previously.[22,23] Each of the primer sequences and PCR conditions are given in Supporting Information Table 1. The PCR was carried out with 0.6 units of AmpliTaq Gold (Applied Biosystems, Foster City, CA) using 7.5 ng of bisulfite-treated DNA. The

Table 1. Thirty regions that were able to discriminate noncancerous liver tissues (N) from normal liver tissues (C)

Region	BAC clone ID	Location	Characteristics	Gene	Cutoff value (%)	DNA methylation status[1]	Sensitivity (%)	Specificity (%)
1	RP11–104J13	1p35.2	Noncoding/CpG island	None	25.5	C > N	80.0	66.7
2	RP11–104J13	1p35.2	Noncoding	None	26.0	C > N	90.0	91.7
3	RP11–104J13	1p35.2	First intron/CpG island	SDC3	34.0	C > N	90.0	91.7
4	RP11–104J13	1p35.2	Noncoding	None	88.9	C < N	100	66.7
5	RP11–52I2	1p33	First exon/CpG island	FOXD2	47.5	C > N	90.0	91.7
6	RP11–29M22	1p12	Intron	PHGDH	73.0	C < N	100	50.0
7	RP11–21K1	2q37.1	Noncoding	None	93.0	C > N	80.0	50.0
8	RP11–109B15	5q33.1	Noncoding	None	12.0	C < N	80.0	83.3
9	RP11–112B7	7p13	First intron/CpG island	CAMK2B	45.0	C > N	20.0	91.7
10	RP11–120E20	11p15.4	Intron	ART5	85.0	C > N	50.0	100
11	RP11–120E20	11p15.4	Intron/SINE repeat	NUP98	95.7	C < N	100	75.0
12	RP11–334E6	11q23.3	First exon/CpG island	C1QTNF5	23.7	C < N	100	25.0
13	RP11–334E6	11q23.3	First intron/CpG island	THY1	12.6	C > N	60.0	83.3
14	RP11–17M17	11q25	First intron	OPCML	74.0	C > N	100	91.7
15	RP11–17M17	11q25	First intron	OPCML	79.0	C > N	100	33.3
16	RP11–17M17	11q25	First intron	OPCML	49.7	C > N	70.0	50.0
17	RP11–319E16	12p13.32	Noncoding	None	79.0	C > N	70.0	58.3
18	RP11–319E16	12p13.32	Noncoding/SINE repeat	None	45.0	C > N	100	50.0
19	RP11–1100L3	12q13.13	UTR	ACVRL1	50.0	C < N	90.0	83.3
20	RP11–1100L3	12q13.13	Promoter/CpG island	GRASP	7.0	C > N	80.0	58.3
21	RP11–799O6	12q13.3	UTR	ZBTB39	40.0	C < N	100	91.7
22	RP11–799O6	12q13.3	Noncoding/SINE repeat	None	89.0	C < N	80.0	100
23	RP11–89M4	16p13.3	Noncoding	None	38.0	C < N	70.0	100
24	RP11–89M4	16p13.3	Intron	LOC342346	69.0	C > N	100	33.3
25	RP11–89M4	16p13.3	Exon/CpG island	MGRN1	51.0	C < N	100	100
26	RP11–89M4	16p13.3	Intron	MGRN1	28.0	C < N	100	50.0
27	RP11–89M4	16p13.3	Intron/CpG island	MGRN1	67.0	C < N	100	100
28	RP11–348B12	19p13.3	Intron/CpG island	KDM4B	44.0	C < N	100	100
29	RP11–348B12	19p13.3	Intron/CpG island	KDM4B	94.8	C < N	100	41.7
30	RP11–348B12	19p13.3	Intron/CpG island	KDM4B	94.0	C > N	50.0	91.7

[1]C > N, when the signal ratio was lower than the cutoff value, the tissue sample was considered to be at high risk for carcinogenesis; C < N, when the signal ratio was higher than the cutoff value, the tissue sample was considered to be at high risk for carcinogenesis.

biotinylated PCR product was captured on streptavidin-coated beads (Streptavidin Sepharose™ High Performance; GE Healthcare, Uppsala, Sweden). Quantitative sequencing was run on the PyroMark Q24 (QIAGEN GmbH) using the Pyro Gold Reagents (QIAGEN GmbH) in accordance with the manufacturer's protocol. For each assay, the setup included positive controls (Epitect methylated human control DNA; QIAGEN GmbH) and negative controls (Epitect unmethylated human control DNA; QIAGEN GmbH). The PCR products were separated electrophoretically on 3% agarose gel and stained with ethidium bromide to confirm that specific products of the appropriate size and no nonspecific products were obtained on amplification. Representative pyrograms are shown in Figure 1.

As outlined in Figure 1, the DNA methylation level (%) at each CpG site is given by the following formula:

$$\text{luminescence strength of cytosine} / (\text{luminescence strength of cytosine} + \text{luminescence strength of thymine}) \times 100.$$

Statistics

Significant differences in DNA methylation levels at each of the CpG sites between groups of samples were analyzed using the Mann-Whitney *U* test. Survival curves of patient groups with HCCs were calculated by the Kaplan–Meier method,

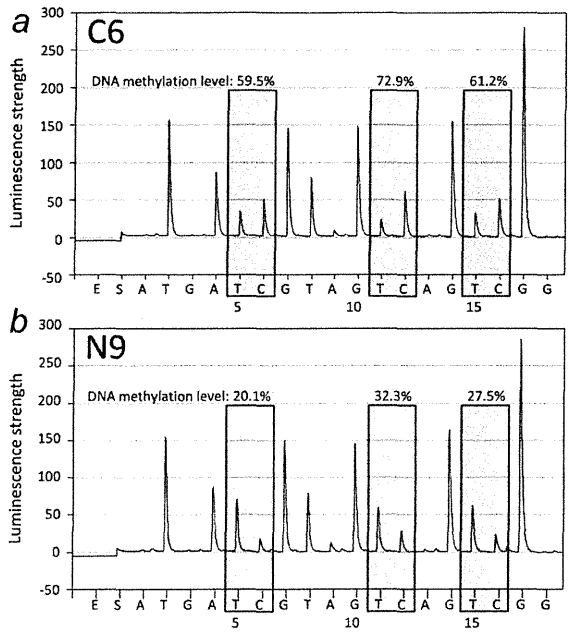

Figure 1. Pyrosequencing DNA methylation analysis. Examples of pyrograms for a sample of normal liver tissue obtained from a patient without HCC (C6) and a sample of noncancerous liver tissue obtained from a patient with HCC (N9) for exon 1 of the *FOXD2* gene (47,677,654, −60, −63 in region 5 in Table 1). Gray columns represent the regions of polymorphic sites after bisulfite modification. *x*-axis indicates dispensation order (time).

and the differences were compared by log-rank test. Differences at $p < 0.05$ were considered significant.

Results

Validation of BAMCA data by pyrosequencing

It has been shown that BAMCA can provide an overview of the DNA methylation tendency of individual large regions among all chromosomes.[13,19] Therefore, using pyrosequencing, we evaluated the DNA methylation levels of all *Xma* I/*Sma* I sites, which yielded less than 2,000 bp PCR products that are effective in BAMCA, on representative BAC clones, which had been identified as indicators for carcinogenetic risk estimation in our previous study.[18] For example, on clone RP11-17M17, there were 10 *Xma* I/*Sma* I sites that were effective in BAMCA (Fig. 2*a*). The average signal ratio by BAMCA of this BAC clone was significantly lower in samples of noncancerous liver tissue obtained from patients with HCCs than in samples of normal liver tissue and was significantly lower in HCCs than in samples of noncancerous liver tissue obtained from patients with HCCs in our previous study.[18] The average DNA methylation levels determined by pyrosequencing of all 10 *Xma* I/*Sma* I sites on this BAC clone in 34 samples of noncancerous liver tissue obtained from patients with HCCs were the same as (*Xma* I/*Sma* I sites i, ii, vii, viii and ix in Fig. 2*a*) or significantly lower than (iii, iv, v, vi and x in Fig. 2*a*) those in 35 samples of normal liver tissue. Moreover, the DNA methylation levels of all *Xma* I/*Sma* I sites in 34 HCCs were significantly lower than those in samples of noncancerous liver tissue obtained from patients with HCCs (i–x in Fig. 2*a*). DNA methylation levels of CpG sites adjacent to the *Xma* I/*Sma* I sites that were quantitatively sequenced using the same sequencing primers tended to be close to the DNA methylation levels of the *Xma* I/*Sma* I sites themselves in each sample, such as iii and iii′ and iv and iv′ in Figure 2*b*. Thus, it was confirmed that BAMCA was able to successfully reveal DNA methylation alterations occurring in a coordinated manner on RP11-17M17. In another BAC clone, RP11-799O6, which was also identified as an indicator for carcinogenetic risk estimation, the average signal ratio obtained by BAMCA was significantly higher in samples of noncancerous liver tissue from patients with HCCs than in samples of normal liver tissue in our previous study.[18] Although the average DNA methylation levels of seven out of 10 *Xma* I/*Sma* I sites, which yielded PCR products of less than 2,000 bp that are effective for BAMCA, by pyrosequencing in samples of noncancerous liver tissue from patients with HCCs were the same as those in samples of normal liver tissue, those of the remaining three *Xma* I/*Sma* I sites in samples of noncancerous liver tissue obtained from patients with HCCs were markedly higher than those in samples of normal liver tissue (data not shown). Thus, pyrosequencing data again validated the BAMCA data for BAC clones identified as indicators for carcinogenetic risk estimation.

Criteria for carcinogenetic risk estimation using liver tissue samples based on pyrosequencing

To identify CpG sites having the largest diagnostic impact, DNA methylation levels of 203 CpG sites were measured by pyrosequencing using primer sets encompassing *Xma* I/*Sma* I sites, which were effective in BAMCA, on the 25 BAC clones on which we based our previous criteria.[18]

On 59 CpG sites, the average DNA methylation levels differed significantly between normal liver tissue and noncancerous liver tissue obtained from patients with HCCs in the learning cohort using Mann-Whitney *U* test ($p < 0.001$). To establish reproducible criteria, 14 CpG sites whose average DNA methylation levels in both normal liver tissue and noncancerous liver tissue obtained from patients with HCCs were less than 10% were omitted from the list of candidate indicators for carcinogenetic risk estimation, taking the characteristics of Pyrosequencing™ technology into consideration.[22] Figure 3*a* shows scattergrams of the DNA methylation levels in samples of normal liver tissue and noncancerous liver tissue obtained from patients with HCCs on representative CpG sites. Using the cutoff values described in each panel, noncancerous liver tissue obtained from patients with

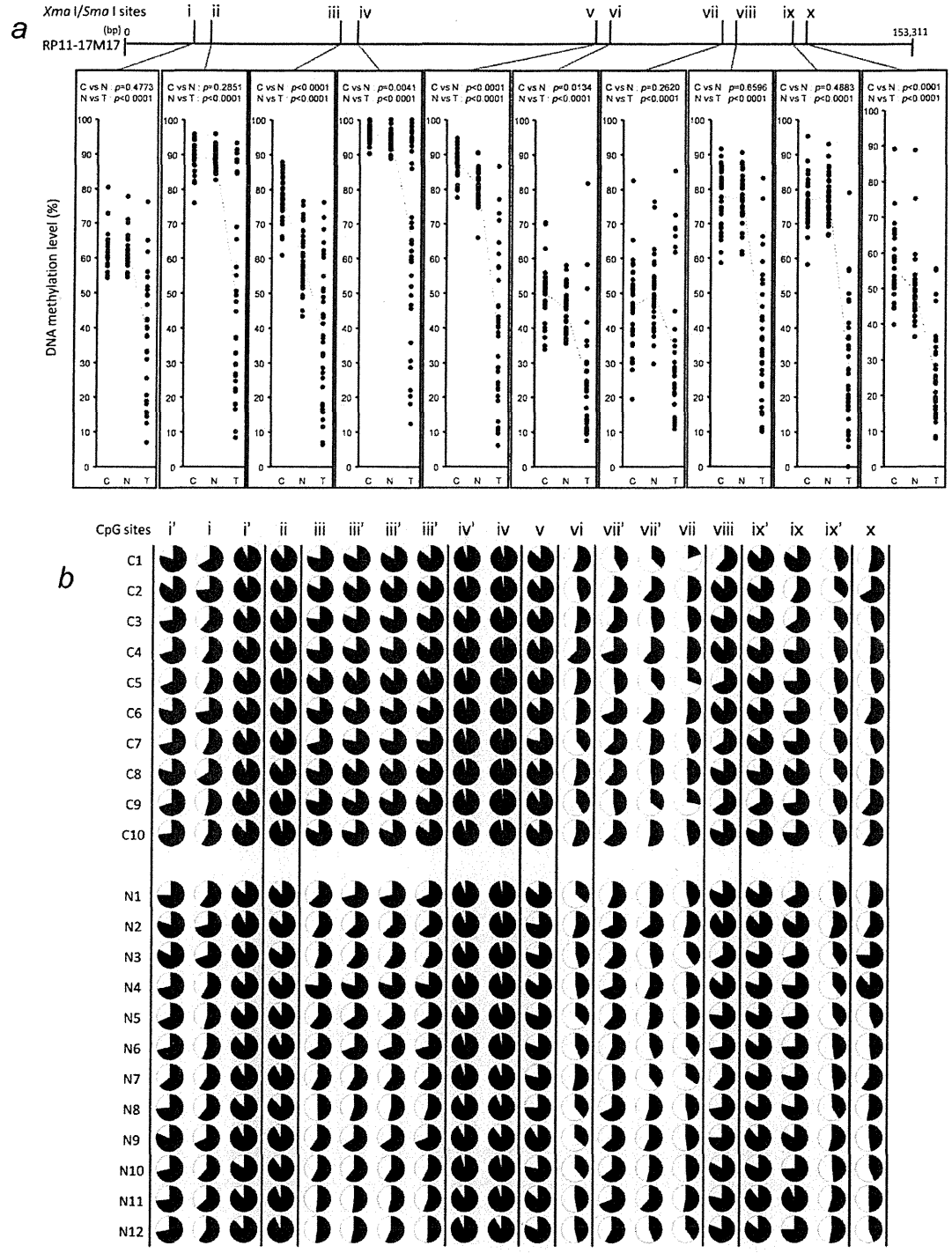

Figure 2. Validation of BAMCA data by pyrosequencing. On RP11-17M17 clone, there were 10 *Xma* I/*Sma* I sites (i–x) that yielded PCR products of less than 2,000 bp that were effective in BAMCA. The average signal ratio obtained by BAMCA for this BAC clone was significantly lower in samples of noncancerous liver tissue obtained from patients with HCCs (N) than in those of normal liver tissue (C) and was significantly lower in HCCs than in N-samples.[18] (*a*) Scattergrams of DNA methylation levels analyzed by pyrosequencing in C-samples (C1–C35), N-samples (N1–N34) and HCCs (T1–T34) on each *Xma* I/*Sma* I site. The average DNA methylation levels obtained by pyrosequencing for all 10 *Xma* I/*Sma* I sites on this BAC clone in 34 N-samples were the same as (on i, ii, vii, viii and ix) or significantly lower than (on iii, iv, v, vi and x) those in 35 C-samples. Moreover, DNA methylation levels in 34 HCCs were significantly lower than those in N-samples (on i–x). (*b*) Pi-charts of DNA methylation levels in C-samples (C1–C10) and N-samples (N1–N12) for each of the CpG sites. CpG sites adjacent to the *Xma* I/*Sma* I site (i, iii, iv, vii and ix), which were quantitatively sequenced using the same sequencing primers, are indicated by i′, iii′, iv′, vii′ and ix′, respectively. White indicates unmethylated cytosine and black indicates methylated cytosine. DNA methylation levels of CpG sites adjacent to the *Xma* I/*Sma* I sites tend to be close to the DNA methylation levels of the *Xma* I/*Sma* I sites themselves, *e.g.*, iii and iii′ and iv and iv′, in each sample.

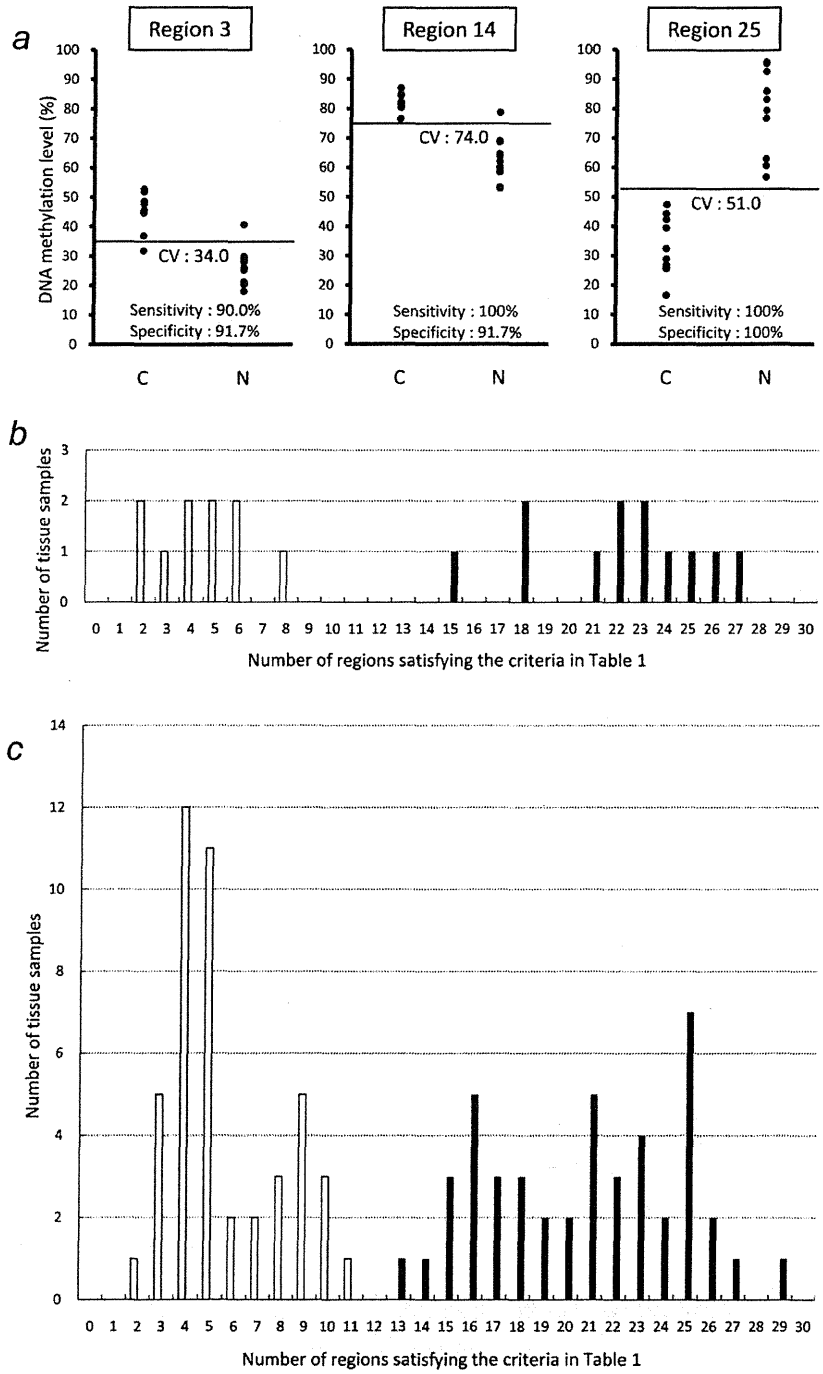

Figure 3. The criteria for carcinogenetic risk estimation based on pyrosequencing. (*a*) Scattergrams of DNA methylation levels in samples of normal liver tissue (C1–C10) and samples of noncancerous liver tissue obtained from patients with HCCs (N1–N12) in the learning cohort for representative regions. Using the cutoff values (CV, %) described in each panel, N-samples in the learning cohort were discriminated from C-samples with sufficient sensitivity and specificity. (*b*) Histogram showing the number of regions satisfying the criteria described in Table 1 in samples C1–C10 (clear columns) and N1–N12 (filled columns). On the basis of this histogram, we judged that when the noncancerous liver tissue satisfied the criteria in Table 1 for 15 or more than 15 regions, it was at high risk of carcinogenesis. (*c*) Validation of the criteria in Table 1 using an additional 90 samples of liver tissue in the validation cohort. All 43 validation samples satisfying the Table 1 criteria for 15 or more regions were N-samples (N13–N36, N38–N41 and N43–N57, filled columns), and 45 of 47 validation samples satisfying the Table 1 criteria for less than 15 regions were C-samples (C11–C55, clear columns). DNA methylation statuses for the 30 regions of N-samples and those of C-samples were completely mutually exclusive in the validation cohort.

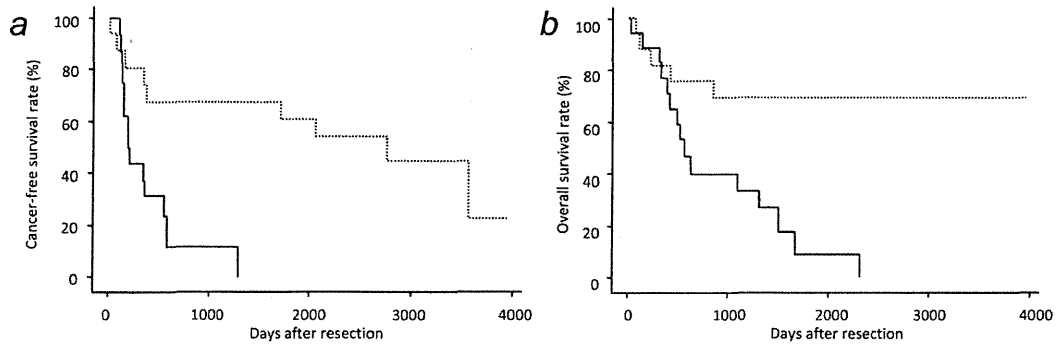

Figure 4. Correlation between DNA methylation status at the precancerous stage and patient outcome. Kaplan–Meier survival curves of patients with HCCs from whom samples N1–N34 were obtained. The cancer-free (*a*; $p = 0.0023$) and overall (*b*; $p = 0.0015$) survival rates of patients with HCCs satisfying the criteria in Table 1 for 23 (the median of the number of regions satisfying the Table 1 criteria) or more than 23 regions in their samples of noncancerous liver tissue ($n = 17$, solid lines) were significantly lower than those of patients with HCCs satisfying the criteria in Table 1 for less than 23 regions ($n = 17$, broken lines).

HCCs in the learning cohort was discriminated from normal liver tissue with sufficient sensitivity and specificity (Fig. 3*a*). On the remaining 45 CpG sites, such discrimination was performed with a sensitivity or specificity of 70% or more than 70%. If several CpG sites were measured using one sequencing primer, one cutoff value was set for the region covered by the sequencing primer using the average DNA methylation levels of the several CpG sites. Then the 30 cutoff values were set for 30 regions including the 45 CpG sites, and their sensitivity and specificity are shown in Table 1. Chromosomal loci and characteristics of the 30 regions (CpG islands or not, exons or introns of specific genes or noncoding regions) are also summarized in Table 1.

A histogram showing the number of regions satisfying the criteria listed in Table 1 for samples C1–C10 and N1–N12 in the learning cohort is shown in Figure 3*b*. On the basis of Figure 3*b*, we finally established that when liver tissue satisfied the criteria in Table 1 for 15 or more regions, it was judged to be at high risk of carcinogenesis. Based on this definition both the sensitivity and specificity for diagnosis of noncancerous liver tissue obtained from patients with HCCs in the learning cohort as being at high risk of carcinogenesis were 100%.

To confirm these criteria, an additional 90 samples of liver tissue were analyzed by pyrosequencing as a validation study (Fig. 3*c*). All of the 43 validation samples satisfying the criteria in Table 1 for 15 or more regions were noncancerous liver tissue obtained from patients with HCCs (N13–N36, N38–N41 and N43–N57), and 45 of the 47 validation samples satisfying the Table 1 criteria for less than 15 regions were normal liver tissue (C11–C55). DNA methylation statuses for the 30 regions of noncancerous liver tissue samples from patients with HCCs and those of normal liver tissue samples were completely mutually exclusive in the validation cohort (Fig. 3*c*), and our criteria enabled diagnosis of noncancerous liver tissue from patients with HCCs in the validation cohort as being at high risk of carcinogenesis with 95.6% sensitivity and 100% specificity.

Clinicopathological significance of DNA methylation status in the 30 regions

To estimate the clinicopathological significance of DNA methylation status in the 30 regions, 34 samples of noncancerous liver tissue from patients with HCCs (N1–N34) in both the learning and validation cohorts for whom follow-up data had been obtained were divided into two groups according to the number of regions satisfying the criteria (≥23 [the median of the number of regions satisfying the Table 1 criteria] regions *vs.* <23 regions). The period covered ranged from 11 to 3,936 days (mean: 1,417 days). The cancer-free and overall survival rates for patients with HCCs satisfying the criteria in Table 1 for 23 or more regions in their noncancerous liver tissue were significantly lower than those of patients with HCCs satisfying the Table 1 criteria for less than 23 regions (Fig. 4, $p = 0.0023$ and $p = 0.0015$, respectively). These data suggested that clinicopathologically valid DNA methylation alterations associated with patient outcome are already present at the precancerous stage.

With respect to all 57 samples of noncancerous liver tissue (N1–N57), the difference in the number of regions satisfying the criteria listed in Table 1 between liver tissue samples showing chronic hepatitis ($n = 26$, 19.6 ± 3.7) and those showing cirrhosis ($n = 31$, 22.0 ± 3.9) was marginal ($p = 0.0206$). For comparison, the DNA methylation levels of 30 regions in 14 additional liver tissue samples (V1–V14) obtained from patients who were infected with HBV or HCV, but who had never developed HCCs, were analyzed by pyrosequencing. The average number of regions satisfying the